Single-shot helicity-independent all-optical switching in Co/Ho multilayers

Y. Peng, G. Malinowski, J. Gorchon, J. Hohlfeld, D. Salomoni, L.D. Buda-Prejbeanu, R.C. Sousa, I.L. Prejbeanu, D. Lacour, Stéphane Mangin, et al.

Single-Shot Helicity-Independent All-Optical Switching in Co/Ho Multilayers

Y. Peng,[1] G. Malinowski,[1,*] J. Gorchon,[1] J. Hohlfeld,[1] D. Salomoni,[2] L.D. Buda-Prejbeanu,[2] R.C. Sousa,[2] I.L. Prejbeanu,[2] D. Lacour,[1] S. Mangin,[1] and M. Hehn[1,†]

[1] *Université de Lorraine, CNRS, Institut Jean Lamour, F-54000 Nancy, France*

[2] *Université Grenoble Alpes, CEA, CNRS, Grenoble INP, SPINTEC, 38000 Grenoble, France*

(Received 28 March 2023; revised 26 May 2023; accepted 7 July 2023; published 31 July 2023)

Single-shot all-optical helicity-independent switching is established in Co/Ho multilayers extending the number of material combinations showing this fascinating property. This ability is studied in wedge-shaped Co/Ho multilayers by varying thicknesses and repetition numbers. Surprisingly, even though the spin-orbit coupling is larger than in Tb and Dy, which should increase the dissipation of angular momentum to the lattice, the pulse duration versus fluence state diagram is close to the one of the Gd-based system.

DOI: 10.1103/PhysRevApplied.20.014068

I. INTRODUCTION

Controlling the local magnetic state in storage media simultaneously with higher-energy efficiency and at a faster timescale is a challenge in modern technologies. In conventional architectures, the magnetic moments are manipulated using magnetic fields and spin currents and the reversal is obtained through a coherent spin precession process at a subnanosecond timescale [1,2].

In the pioneering work by Beaurepaire *et al.* [3], femtosecond (fs) laser pulse has been demonstrated to demagnetize the Ni thin films within less than 1 ps opening the field of ultrafast magnetization manipulation. Since then, considerable attention has been paid to the interactions between fs laser pulse and spins due to the great potential applications in ultrafast spintronics. In particular, all-optical switching (AOS) of magnetization has been demonstrated experimentally in the rare earth-transition metal (RE-TM) alloy $Gd_xFe_yCo_{1-x-y}$ using a fs laser pulse without the aid of magnetic field [4]. This intriguing experimental observation is highly significant for generating smaller, faster, and less energy costly technological implementations in information processing and recording devices. Many works have been carried out in the area of AOS, including its observation in a wide variety of ferromagnetic or ferrimagnetic materials [5,6], and the exploration of the parameters for the achievements of AOS such as the fluence, helicity, and duration of laser pulses [7–9]. To date, both all-optical helicity-dependent (AOHDS) and independent (AOHIS) magnetization switching were found. AOHDS is quite general in various ferrimagnetic and ferromagnetic materials [10–13]. In contrast, AOHIS has been, for a long time, observed only in Gd-based RE-TM alloys [14,15] or multilayers [16–18]. Recently, it was discovered that it can also be achieved in the RE-free Heusler alloy Mn_2Ru_xGa [19–21] or multilayers including Tb, Tb-Co, Dy-Co, Tb-Fe and a TM layer made of Co, Fe, Co-Fe-B, and Py as well [22–24]. In this last class of multilayers, the pulse duration and fluence state diagram and the reversal dynamics contrast with the one observed for Gd-based compounds suggesting that the reversal process differs [24]. Indeed, the critical reversal fluence does not depend on the laser pulse duration and the magnetization reversal occurs on a sub-ns timescale while critical reversal fluence depends on the laser pulse duration and reversal occurs on the ps timescale in the case of Gd-based compounds. Since a clear view of the reversal process is still missing, additional information from the experiment is welcome. Here we report results substituting the RE with holmium. This RE has the largest total momentum [25] and a higher spin-orbit coupling than Tb and Dy [26]. We therefore expect to strengthen the effects observed for Tb and Dy.

In this study, we experimentally demonstrate AOHIS in [Co/Ho] multilayer stacks with perpendicular magnetic anisotropy. Surprisingly, even though the spin-orbit coupling is larger than in Tb and Dy [26], which should increase the dissipation of angular momentum to the lattice, the pulse duration and fluence state diagram is closer to the one of the Gd-based system. The study of this system could help to bridge the single-pulse reversal processes observed, on one hand, in Gd based and, on the other hand, in the Tb- or Dy-based heterostructures.

*gregory.malinowski@univ-lorraine.fr
†michel.hehn@univ-lorraine.fr

II. EXPERIMENTAL RESULTS

Wedge-shaped glass/Ta(5)/Pt(5)/[Co(wedge, $0.5t_1$–$1.5t_1$)/Ho(wedge, $0.5t_2$–$1.5t_2$)]$_N$/Pt(1)/Ta(5) multilayers (thickness in nm) were fabricated by dc magnetron sputtering, where N indicates the repetition numbers of Co/Ho bilayers [schematic given in Fig. 1(a)]. Co and Ho layers are wedged in the same direction, resulting in a constant thickness ratio (t_1: t_2) all over the wedge. In the following, the thickness of Co and Ho varies from 0.4 to 1.2 nm, and 0.45 to 1.35 nm, respectively, resulting in a 1:1.1 thickness ratio of the thickness of Co and Ho monolayer. The magnetic hysteresis loops of the samples are characterized by static magneto-optic Kerr effect (MOKE) at room temperature with a magnetic field applied perpendicular to the film plane. All samples are perpendicular to film magnetization and exhibit high squareness of the hysteresis loops and 100% remanence [Fig. 1(b)]. The positive sign of the Kerr rotation at high positive field shows that the multilayer is dominated by the Co sublattice, although the thickness of the Ho layer is thicker than the Co layer. This is mainly ascribed to the low Curie temperature of the Ho element, which is around 19 K [27].

The saturation magnetization, M_S, and coercive field, H_C, have the characteristic variations as a function of temperature, T, shown by ferrimagnetic alloys. This is expected from the antiferromagnetic (AF) exchange coupling between Co and Ho at the Co/Ho interface. As shown in Fig. 1(c), the M_S versus T curve shows a compensation temperature T_{comp} at which the magnetic moments of the Co and Ho layers are equal, resulting in a zero net magnetization. Below T_{comp}, the net magnetization is dominated by Ho while it is dominated by Co above T_{comp}. At T_{comp}, H_C diverges since M_S equals zero.

Ti:sapphire femtosecond-laser source and regenerative amplifier were used for the pump laser beam in AOS measurement. Wavelength and repetition rate of the femtosecond laser are 800 nm and 5 kHz, respectively. Figure 1(d) shows the result of the measurement performed on the [Co(0.46)/Ho(0.52)]$_4$ stack, in which the sample is exposed to four subsequent laser pulses with laser fluence $F = 5.22$ mJ/cm^2. We can clearly observe a switched area after the first laser pulse. After the second pulse, the magnetic moments are the reverse to the initial state, indicating a good sign of toggle magnetization switching. Similar results are obtained in samples with slightly thicker thicknesses [see [Co(0.6)/Ho(0.7)]$_4$]. By further increasing the thicknesses of Co and Ho, the magnetization switching area after the first laser pulse becomes much less smooth [see [Co(0.81)/Ho(0.91)]$_4$]. Moreover, the subsequent laser pulses lead to the formation of a multidomain structure, suggesting the loss of magnetization toggle switching when the thickness of Co and Ho reaches 0.8 and 0.9 nm, respectively. The shape of the domain after

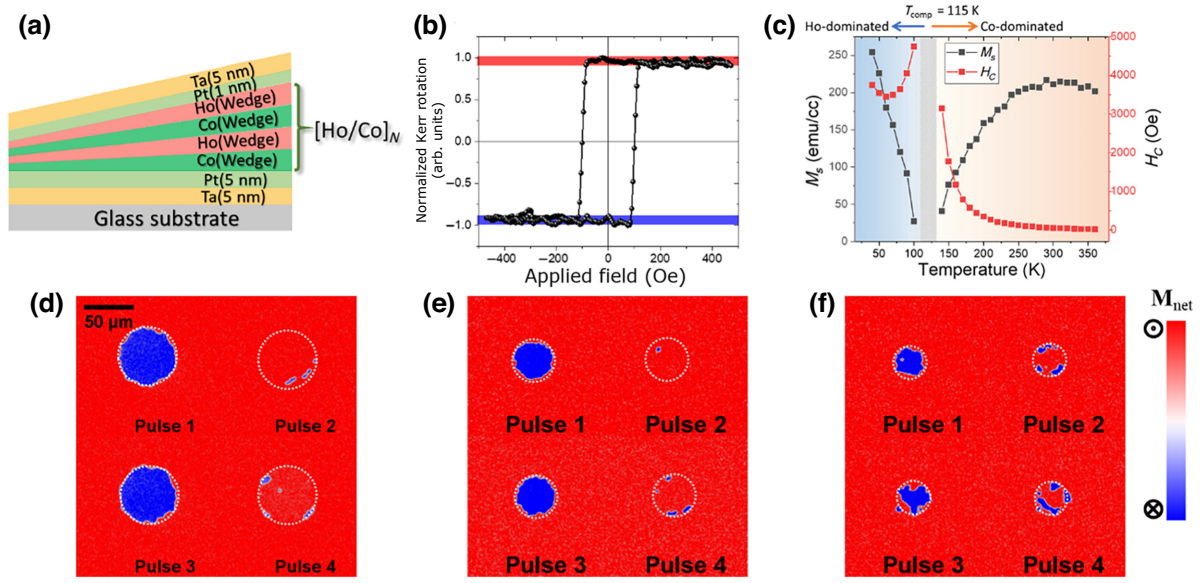

FIG. 1. (a) Schematic of the wedged [Co/Ho]$_N$. The Co and Ho layers are wedged in the same direction with graded monolayer thickness spanning $0.5t_1 < t_{\text{Co}} < 1.5t_1$ and $0.5t_2 < t_{\text{Ho}} < 1.5t_2$. The square brackets contain the bilayer structure that is repeated N times within each sample. (b) Polar magneto-optical Kerr effect measurement performed at room temperature on [Co(0.46)/Ho(0.52)]$_4$; (c) saturation magnetization M_s and coercivity H_c as a function of temperature, which is performed on the same stack as (b). AOS measurements performed on [Co/Ho]$_4$ stacks with different Co and Ho thicknesses. (d) [Co(0.46)/Ho(0.52)]$_4$; (e) [Co(0.6)/Ho(0.7)]$_4$; (f) [Co(0.81)/Ho(0.91)]$_4$ (thickness in nm). The dotted circle regions correspond to the spots where the structure is excited by each single laser pulse (fluence 5.22 mJ/cm^2, pulse duration 50 fs). Red and blue colors represent the net magnetization pointing up and down.

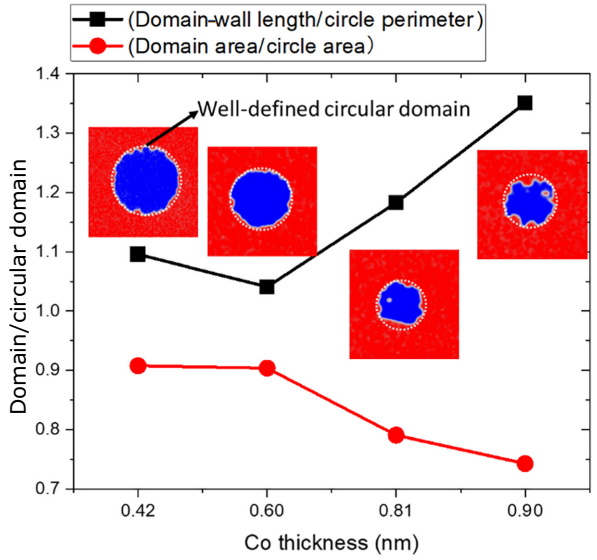

FIG. 2. Analysis of the domain wall length and domain area compared to a well-defined circular domain. Insets are the domain patterns after the first pulse for different Co thickness (the thickness ratio of Co and Ho is constant and equal to 1: 1.1). An increase of the domain wall length is obviously associated to a decrease of the domain area.

an odd number of pulses is not a 100% well-defined circle and some small domains at the rim appear after an even number of pulses.

We made a statistical analysis of the area of the reversed domain and domain wall length divided by the values, which would be obtained for a well-defined circular domain. The ratios as a function of Co thickness are reported in Fig. 2. It exhibits that domain area ratio is below 1 and becomes smaller while domain wall length ratio is above 1 and becomes larger with increasing the thickness of Co. While the analysis of this result is beyond the scope of this paper, we could attribute it to a change of texture in the multilayer with layer thickness or change of size of stable domains through the variation of saturation magnetization, anisotropy, or effective exchange coupling. We conclude that the thickness of Co and Ho layers are critical to observe AOHIS and they have to be less than 0.8 and 0.9 nm, respectively, when repetition number $N = 4$. Otherwise, the domain shape becomes dendritic and the magnetization switching becomes randomized.

Based on the above results, we fixed the thicknesses of Co layers ranging from 0.25 to 0.75 nm and Ho layers ranging from 0.28 to 0.83 nm, while keeping the same ratio fixed to 1:1.1 and deposited a series of samples with repetition of the bilayer varies from 2 to 5. As shown in Fig. 3, all the samples show nice single-pulse switching. For $N = 2$, below a certain Co (Ho) single-layer thickness of approximately 0.56 nm (0.62 nm), only the multidomain state is observed. For larger Co and Ho thicknesses, a clear toggle switching is observed. For $N = 3$, this minimum thickness of Co (Ho) monolayer extends to 0.31 nm (0.34 nm). For $N = 4$ and $N = 5$, the reversal occurs for all the thicknesses in the wedge.

Increasing the laser fluence leads to the appearance of a multidomain state at the center of the spot while an outer ring maintains the single-shot switching. As a result, we can define F_{switch} and F_{multi}, the minimum fluence to get the single-shot switching and to get the multidomain state, respectively. We investigate the layer thickness dependence of F_{switch} and F_{multi} for a fixed pulse duration of 50 fs. In Fig. 3(c), we can clearly see that F_{switch} increases almost linearly with the total thickness of the multilayer. In the case of F_{multi}, the variation with thickness is not

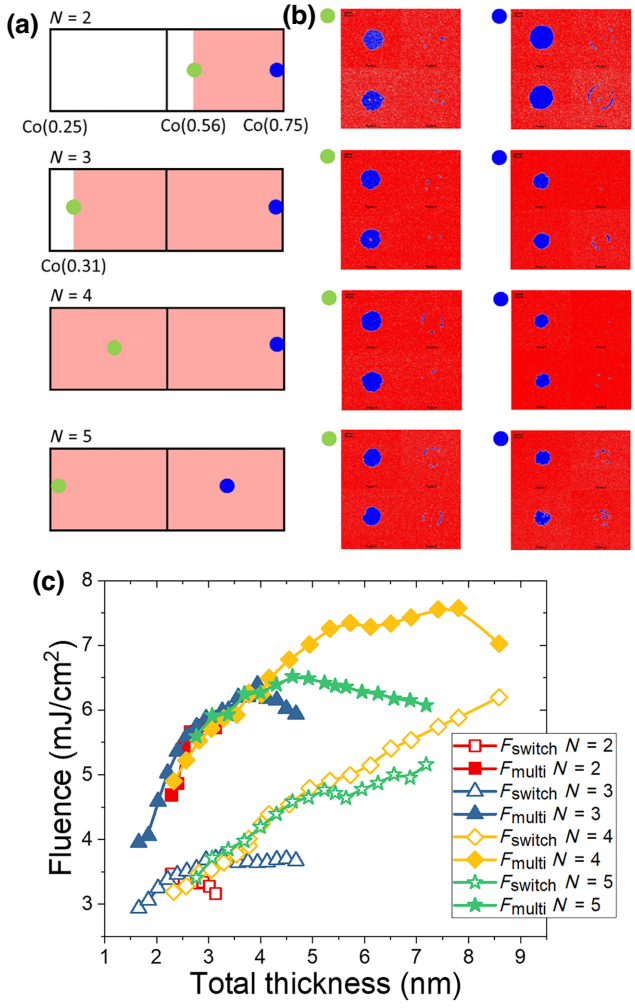

FIG. 3. (a) The range of Co and Ho layer thicknesses (shown by light red color) where single-shot switching occurs in $[\text{Co/Ho}]_N$ multilayers, where the repetition number of the Co/Ho bilayer N equals to 2, 3, 4, 5, respectively. (b) Single-pulse reversal in V/Ta(5)Pt(5)$[\text{Co}(0.5)/\text{Ho}(0.55)]_N$/Pt(1)Ta(5) at 3.75 mJ/cm^2 and pulse duration of 50 fs measured at location of blue and green dot. In each image, first line pulse 1 and 2, second line pulse 3 and 4. (c) Variation of F_{switch} and F_{multi} as a function of total Co/Ho thickness for pulse duration of 50 fs.

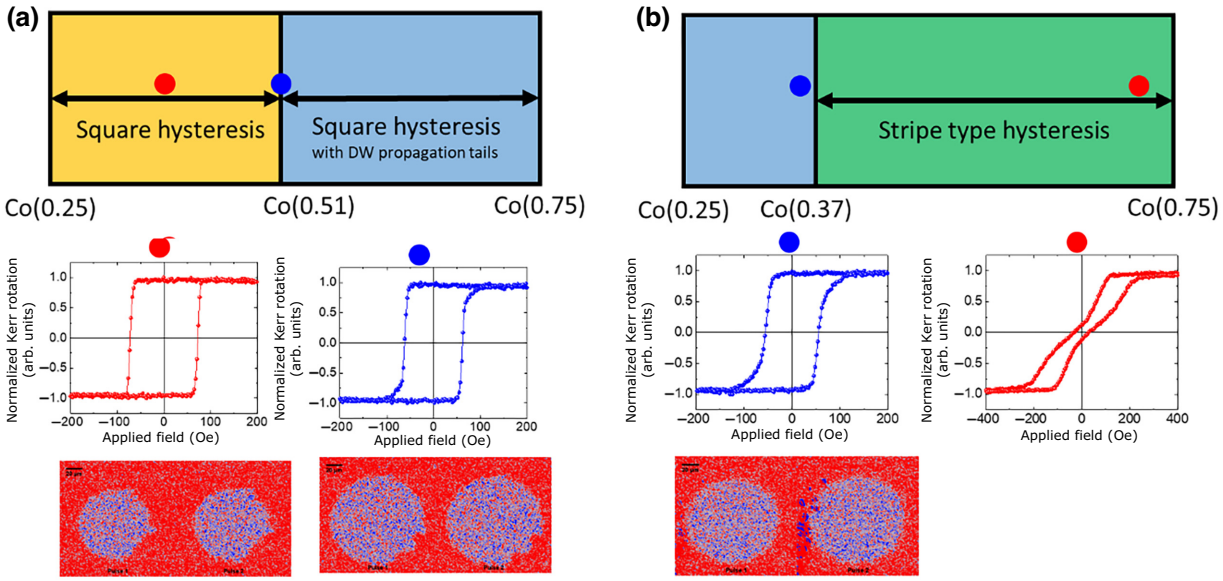

FIG. 4. Single-pulse reversal in (a) V/Ta(5)Pt(5)[Co(0.5)/Ho(0.55)]$_4$/Pt(1)Ta(5) and (b) V/Ta(5)Pt(5)[Co(0.5)/Ho(0.55)]$_5$/Pt(1)Ta(5) after anneal. Top line: region of space showing different hysteresis loops: orange – square hysteresis, blue – remanence equal to one with high field tails, green – hysteresis loop characteristic of stripe domains. Middle line: hysteresis loop measured at location of blue and red dot, characteristic of the three regions of space. Bottom line: Kerr image after first and second laser shot pulse with pulse duration of 50 fs (blue areas are magnetized down, red areas are magnetized up).

monotonic: while it increases when the total thickness is below 4.5 nm, it saturates and can even decrease when thickness increases. As a result, when thickness is too high, $F_{\text{multi}} < F_{\text{switch}}$ and only a demagnetized state is observed. We think that this trend is directly linked to the variation of the stable domain size with thickness in thin film with PMA: in the range of thickness studied here, the size of domains decreases when thickness increases. As a result, even if a switch of magnetization occurs, a stabilization of small domains with sizes less than the spot size occurs during thermal cooling in the thickest film leading to a demagnetized state. As a result, the best thickness range for HIAOS to be observed is between 2 and 4.5 nm.

Another piece of evidence that the magnetic properties play a role on the single-pulse switching is reported in Fig. 4. Samples measured in Fig. 3 with $N = 4$ and 5 have been annealed at 200 °C during 1 h without any applied field. While PMA is conserved for all thicknesses, a large variety of hysteresis loops could be observed, ranging from square hysteresis to hysteresis loop characteristic of stripe and bubble domains. In all cases, a Co-dominant response is kept, as before the annealing. Kerr images after the first and second laser shot pulse with pulse duration of 50 fs reveal that single-pulse switching no longer holds and is replaced by the formation of small domains and a demagnetized state. The effect of annealing on the interfaces and crystalline structure has to be more deeply checked. However, if interface alloying is considered, a decrease of saturation magnetization is expected by the increase of Ho momentum. So, only a decrease of the domain-wall energy can explain the behavior observed by a decrease of the exchange constant or of the magnetic anisotropy.

To gain further insight of the dependence of magnetization switching on the laser pulse parameters, the state diagram describing the evolution of both F_{switch} and F_{multi} as a function of laser pulse durations has been measured (Fig. 5). In the state diagram, three regions including AOHIS, multidomain state or no reversal, are categorized depending on the various magnetic states obtained after laser pulse irradiation. At the 35 fs, the laser fluence window allowing for AOHIS is widest. By increasing the pulse length, F_{switch} is increased, while F_{multi} is almost constant. Ideally, once $F_{\text{switch}} = F_{\text{multi}}$, the maximum pulse duration τ_{max} for which AOHIS is reached. Here, the value of τ_{max} is around 1.1 ps above which only the demagnetized multidomain structures can be achieved. This leads to an approximately triangle shape of switching area, which is very similar with the one reported in $Gd_xFe_yCo_{1-x-y}$ alloys [14], even though the samples do not host Gd. In contrast, the samples host a heavy RE with strong spin-orbit coupling, similar to Tb and Dy but the state diagram of Co/Ho is significantly different with the one reported in multilayers including Tb, Tb-Co, Dy-Co, Tb-Fe and a TM layer made of Co, Fe, Co-Fe-B and Py as well [22–24]. As a result, the current understanding of the HIAOS process in Gd that low spin-orbit and damping materials are required does not depict the behavior of Ho that needs to be understood. It suggests that other parameters like demagnetization times, Curie temperature have to be explored to gain more insights into the process.

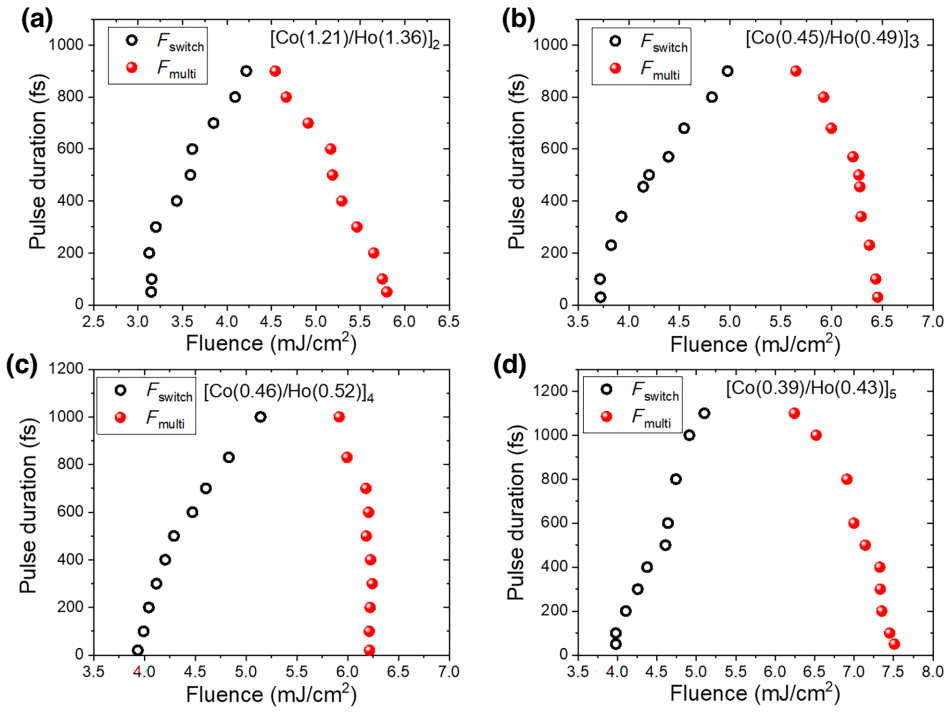

FIG. 5. State diagram: switching fluence F_{switch} (open black circle) and multidomain fluence F_{multi} (full red sphere) as a function of the pulse duration for a single linearly polarized laser pulse. (a) $[Co(1.21)/Ho(1.36)]_2$; (b) $[Co(0.45)/Ho(0.49)]_3$; (c) $[Co(0.46)/Ho(0.52)]_4$; (d) $[Co(0.39)/Ho(0.43)]_5$.

III. CONCLUSIONS

In this study, we establish single-shot all-optical helicity-independent switching is Co/Ho multilayers extending the number of material combinations showing this fascinating property. By varying the thicknesses of Co and Ho, the number of repetitions of the bilayers, we show that F_{switch} increases with the total thickness, while $F_{switch} - F_{multi}$, the windows of fluence for which AOHIS occurs, has an optimum in total thickness ranging from 2 to 4.5 nm. The state diagram describing the evolution of both F_{switch} and F_{multi} as a function of laser pulse duration is very similar to that reported in $Gd_xFe_yCo_{1-x-y}$ alloys, while the samples do not host Gd. While with the use of Ho we reinforced the spin-orbit coupling and the total magnetic momentum with respect to Tb and Dy, we expected to strengthen the reversal characteristics in Tb- and Dy-based compounds. The further study of Ho-based materials could help to understand the difference in behavior in Gd-based materials, on one hand, and in Tb- or Dy-based heterostructures, on the other hand. In particular, the study of their reversal dynamics, beyond the scope of this paper, could help to answer this problem.

ACKNOWLEDGMENTS

We acknowledge financial support from the ANR (ANR-17-CE24-0007 UFO project), the Region Grand Est through its FRCR call (NanoTeraHertz and RaNGE projects), by the impact project LUE-N4S part of the French PIA project "Lorraine Université d'Excellence", reference ANR-15IDEX-04-LUE and by the "FEDER-FSE Lorraine et Massif Vosges 2014-2020", a European Union Program. D.S. has received funding from the European Union's Horizon 2020 research and innovation programme under Marie Skłodowska-Curie Grant Agreement No. 861300 (COMRAD).

[1] H. Liu, D. Bedau, D. Backes, J. A. Katine, J. Langer, and A. D. Kent, Ultrafast switching in magnetic tunnel junction based orthogonal spin transfer devices, Appl. Phys. Lett. **97**, 242510 (2010).

[2] H. Zhao, B. Glass, P. K. Amiri, A. Lyle, Y. Zhang, Y.-J. Chen, G. Rowlands, P. Upadhyaya, Z. Zeng, J. A. Katine, J. Langer, K. Galatsis, H. Jiang, K. L. Wang, I. N. Krivorotov, and J.-P. Wang, Sub-200 ps spin transfer torque switching in in-plane magnetic tunnel junctions with interface perpendicular anisotropy, J. Phys. D: Appl. Phys. **45**, 025001 (2012).

[3] E. Beaurepaire, J.-C. Merle, A. Daunois, and J.-Y. Bigot, Ultrafast Spin Dynamics in Ferromagnetic Nickel, Phys. Rev. Lett. **76**, 4250 (1996).

[4] C. D. Stanciu, F. Hansteen, A. V. Kimel, A. Kirilyuk, A. Tsukamoto, A. Itoh, and Th. Rasing, All-Optical Magnetic Recording with Circularly Polarized Light, Phys. Rev. Lett. **99**, 047601 (2007).

[5] A. V. Kimel and M. Li, Writing magnetic memory with ultrashort light pulses, Nat. Rev. Mater. **4**, 189 (2019).

[6] C. Wang and Y. Liu, Ultrafast optical manipulation of magnetic order in ferromagnetic materials, Nano Convergence **7**, 35 (2020).

[7] T. A. Ostler, *et al.*, Ultrafast heating as a sufficient stimulus for magnetization reversal in a ferrimagnet, Nat. Commun. **3**, 666 (2012).

[8] M. S. El Hadri, M. Hehn, P. Pirro, C.-H. Lambert, G. Malinowski, E. E. Fullerton, and S. Mangin, Domain size criterion for the observation of all-optical helicity-dependent switching in magnetic thin films, Phys. Rev. B **94**, 064419 (2016).

[9] H. Hamamera, F. Souza Mendes Guimarães, M. dos Santos Dias, and S. Lounis, Polarisation-dependent single-pulse ultrafast optical switching of an elementary ferromagnet, Commun. Phys. **5**, 16 (2022).

[10] S. Mangin, M. Gottwald, C.-H. Lambert, D. Steil, P. Lin, M. Hehn, S. Alebrand, M. Cinchetti, G. Malinowski, S. Fainman, M. Aeschliman, and E. E. Fullerton, Engineered materials for all-optical helicity-dependent magnetic switching, Nat. Mater. **13**, 287 (2014).

[11] C.-H. Lambert, S. Mangin, B. S. D. Ch. S. Varaprasad, Y. K. Takahashi, M. Hehn, M. Cinchetti, G. Malinowski, K. Hono, Y. Fainman, M. Aeschlimann, and E. E. Fullerton, All-optical control of ferromagnetic thin films and nanostructures, Science **345**, 1337 (2014).

[12] F. Cheng, Z. Du, X. Wang, Z. Cai, L. Li, C. Wang, A. Benabbas, P. Champion, N. Sun, L. Pan, and Y. Liu, All-optical helicity-dependent switching in hybrid metal–ferromagnet thin films, Opt. Mater. **8**, 2000379 (2020).

[13] A. Ciuciulkaite, K. Mishra, M. V. Moro, I.-A. Chioar, R. M. Rowan-Robinson, S. Parchenko, A. Kleibert, B. Lindgren, G. Andersson, C. S. Davies, A. Kimel, M. Berritta, P. M. Oppeneer, A. Kirilyuk, and V. Kapaklis, Magnetic and all-optical switching properties of amorphous Tb_xCo_{100-x} alloys, Phys. Rev. Mater. **4**, 104418 (2020).

[14] J. Wei, B. Zhang, M. Hehn, W. Zhang, G. Malinowski, Y. Xu, W. Zhao, and S. Mangin, All-optical Helicity-Independent Switching State Diagram in Gd-Fe-Co Alloys, Phys. Rev. Appl. **15**, 054065 (2021).

[15] M. Beens, M. L. M. Lalieu, A. J. M. Deenen, R. A. Duine, and B. Koopmans, Comparing all-optical switching in synthetic-ferrimagnetic multilayers and alloys, Phys. Rev. B **100**, 220409(R) (2019).

[16] M. L. Lalieu, M. J. G. Peeters, S. R. R. Haenen, R. Lavrijsen, and B. Koopmans, Deterministic all-optical switching of synthetic ferrimagnets using single femtosecond laser pulses, Phys. Rev. B **96**, 220411(R) (2017).

[17] P. Z. Li, J. W. van der Jagt, M. Beens, J. Hintermayr, M. A. Verheijen, R. Bruikman, B. Barcones, R. Juge, R. Lavrijsen, D. Ravelosona, and B. Koopmans, Enhancing all-optical switching of magnetization by He ion irradiation, Appl. Phys. Lett. **121**, 172404 (2022).

[18] L. D. Wang, Y. L. W. van Hees, R. Lavrijsen, W. S. Zhao, and B. Koopmans, Enhanced all-optical switching and domain wall velocity in annealed synthetic-ferrimagnetic multilayers, Appl. Phys. Lett. **117**, 022408 (2020).

[19] C. Banerjee, N. Teichert, K. E. Siewierska, Z. Gercsi, G. Y. P. Atcheson, P. Stamenov, K. Rode, J. M. D. Coey, and J. Besbas, Single pulse all-optical toggle switching of magnetization without gadolinium in the ferrimagnet Mn_2Ru_xGa, Nat. Commun. **11**, 4444 (2020).

[20] C. S. Davies, G. Bonfiglio, K. Rode, J. Besbas, C. Banerje, P. Stamenov, J. M. D. Coey, A. V. Kimel, and A. Kirilyuk, Exchange-driven all-optical magnetic switching in compensated 3d ferrimagnets, Phys. Rev. Res. **2**, 032044(R) (2020).

[21] C. Banerjee, K. Rode, G. Atcheson, S. Lenne, P. Stamenov, J. M. D. Coey, and J. Besbas, Ultrafast Double Pulse All-Optical Reswitching of a Ferrimagnet, Phys. Rev. Lett. **126**, 177202 (2021).

[22] L. Avilés-Félix, L. Álvaro-Gómez, G. Li, C. S. Davies, A. Olivier, M. Rubio-Roy, S. Auffret, A. Kirilyuk, A. V. Kimel, T. Rasing, L. D. Buda-Prejbeanu, R. C. Sousa, B. Dieny, and I. L. Prejbeanu, Integration of Tb/Co multilayers within optically switchable perpendicular magnetic tunnel junctions, AIP Adv. **9**, 125328 (2019).

[23] L. Avilés-Félix, A. Olivier, G. Li, C. S. Davies, L. Álvaro-Gómez, M. Rubio-Roy, S. Auffret, A. Kirilyuk, A. V. Kimel, Th. Rasing, L. D. Buda-Prejbeanu, R. C. Sousa, B. Dieny, and I. L. Prejbeanu, Single-shot all-optical switching of magnetization in Tb/Co multilayer-based electrodes, Sci. Rep. **10**, 5211 (2020).

[24] Y. Peng, D. Salomoni, G. Malinowski, W. Zhang, J. Hohlfeld, L. D. Buda-Prejbeanu, J. Gorchon, M. Vergès, J. X. Lin, D. Lacour, R.C. Sousa, I. L. Prejbeanu, S. Mangin, and M. Hehn, In plane reorientation induced single laser pulse magnetization reversal in rare-earth based multilayer, arXiv:2212.13279. (2023), to be published.

[25] J. Zhou and G. A. Fiete, Rare earths in a nutshell, Phys. Today **73**, 66 (2020).

[26] K. V. Shanavas, Z. S. Popovic, and S. Satpathy, Theoretical model for Rashba spin-orbit interaction in electrons, Phys. Rev. **90**, 165108 (2014).

[27] B. L. Rhodes, S. Legvold, and F. H. Spedding, Magnetic properties of holmium and thulium metals, Phys. Rev. **109**, 1547 (1958).